AIMS Materials Science, 10(4): 589–603.
DOI: 10.3934/matersci.2023033
Received: 25 May 2023
Revised: 30 June 2023
Accepted: 06 July 2023
Published: 27 July 2023

http://www.aimspress.com/journal/Materials

Perspective

Study of the structure and mechanical properties of composites used in the oil and gas industry

Peter Rusinov*, Zhesfina Blednova, Anastasia Rusinova, George Kurapov and Maxim Semadeni

Kuban State Technological University, Krasnodar, Russia

*** Correspondence:** Email: ruspiter5@mail.ru; Tel.: +7-908-690-8810.

Abstract: This article describes the structure and properties of the developed hybrid composite Hastelloy X (NiCrFeMo)-AlMoNbTaTiZr-cBNSiCNiAlCo. The composite was obtained by the high velocity oxygen fuel spraying (HVOF) method in a protective atmosphere with a subsequent high-temperature thermomechanical treatment. In order to obtain new information about the structure, we studied the metallophysical properties of the composite using electron microscopy and X-ray diffraction analysis, as well as the mechanical properties and phase composition. We studied the influence of high-energy mechanical processing of high-entropic and ceramic materials on the structural-phase state and composite quality. We determined the optimal technological parameters of HVOF in a protective atmosphere, followed by a high-temperature thermomechanical treatment. Additionally, we optimized these parameters to form a hybrid composite providing the highest adhesion and low porosity. Moreover, we investigated the microhardness of the composite layers. On the basis of complex metallophysical studies, we examined the composite formation. In order to determine the endurance limit in comparison to various other composite materials, we carried out cyclic endurance tests of the developed materials.

Keywords: composite materials; high-entropic materials; surface modification; multi-cycle fatigue; cyclic durability

1. Introduction

In the modern industry, under conditions of intense global competition, increased requirements are imposed on products; they are expected to have proper structure, chemical composition, high mechanical properties, and geometric dimensions [1–4]. Given the decisive role of the surface layers, the problem of increasing the operational characteristics and increasing reliability and service life can be successfully solved at the finishing stage of processing. This processing is based on a layered synthesis using combined (hybrid), function-oriented macro-, micro-, and nanotechnology. These technologies are a new type of organizational and technological form of additive technologies [5–9].

The multilayer hybrid composite material is characterized by greater energy absorption than single-layer materials [10–14]. Its rate of microcrack propagation is decreased in the layers, which has a gradient in the phase composition and layer thickness. The material has high adhesive properties of the constituent layers and the base, as well as guaranteed technological features and good selection of bonding layers [7–9,15,16]. The most promising is the concept of multilayer material architecture, where each layer has its own functional purpose. A multilayer surface composition allows a set of extremely important functions related to an increased resistance of the composition to fatigue failure under cyclic loads, which causes fatigue cracks [17–20]. The composition helps to slow down or block failure under loading due to phase transformations in the material [21–27].

Functionalization and intellectualization of products is a promising direction in layered synthesis technologies. These processes are carried out using high-entropic and ceramic materials. Increasingly expanding the use of high-entropic and ceramic materials in engineering is connected with their extremely wide functional-mechanical characteristics, including the following: high strength and damping properties, thermomechanical reliability and durability, and wear and corrosion resistance [9,15,23].

The aim of the work is to develop and study the structure and properties of the high-entropic layered heat-resistant composite Hastelloy X (NiCrFeMo)-AlMoNbTaTiZr-cBNSiCNiAlCo. Additionally, we aim to develop optimal technological parameters of its production and to evaluate the specified structural and mechanical properties for details, units and assemblies working in the oil and gas industry.

To achieve the goal, we formulated the following tasks:

-To study the influence of high-energy mechanical processing of powders AlMoNbTaTiZr and cBNSiCNiAlCo on the structural-phase state and quality of the composite material obtained by HVOF (high velocity oxygen fuel spraying) in a protective atmosphere with subsequent high temperature thermomechanical processing (HTTP), which provides functional and mechanical properties of details, units and assemblies used in the oil and gas industry;

-To develop optimal technological parameters of HVOF in a protective atmosphere with subsequent HTTP to form composite Hastelloy X (NiCrFeMo)-AlMoNbTaTiZr-cBNSiCNiAlCo, ensuring reliable adhesion and cohesion;

-To establish the formation procedure for the composite Hastelloy X(NiCrFeMo)-AlMoNbTaTiZr-cBNSiCNiAlCo, on the basis of complex metallophysical studies;

-To study the influence of thermal and high-temperature thermomechanical processing on the functional and mechanical properties of the Hastelloy X (NiCrFeMo)-AlMoNbTaTiZr-cBNSiCNiAlCo;

-And to investigate the influence of cyclic loading in the region of multicyclic fatigue on the structural-mechanical properties of the Hastelloy X (NiCrFeMo)-AlMoNbTaTiZr-cBNSiCNiAlCo composites.

2. Materials and methods

Figure 1 shows a diagram for the processes that determine the formation and performance properties of the composites. The choice of the composition architecture "base-layer of HEAs-layer of combined ceramics" depends on its functional purpose. The surface layers of products working in the oil and gas industry are subjected to external force, temperature, and corrosion effects, and must ensure strength, reliability and survivability in operating conditions. The main factors, which determine the reliability and survivability of the composition, are high adhesion at both the "composite layer-base" interface and between the layers; the "architecture" of the surface composition, which prevents cracks and creates barriers to their propagation, ensures the inhibition of the cracks' propagation.

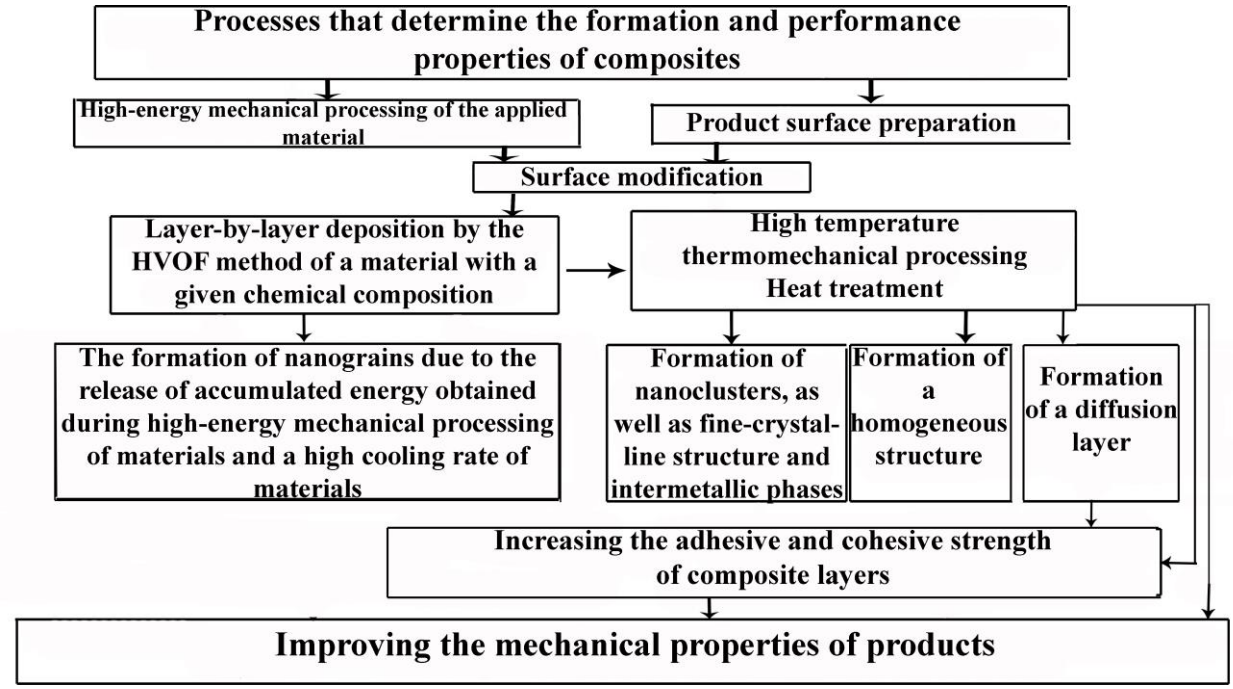

Figure 1. Scheme of processes that determine the formation and performance properties of composites.

The methodology of hybrid composite materials was carried out in accordance with the five-link paradigm of materials science, in the composition-structure-technology- properties-material relationship. The chemical composition of the composite material is chosen considering the operational requirements to the details, units, and aggregates used in the oil and gas industry. By providing the necessary functional-mechanical properties, we chose the proper equipment and developed the technology to form the material structure.

The Hastelloy X (NiCrFeMo) is used as the base of the composition, and the AlMoNbTaTiZr powder was used as the lower functional layer. The cBNSiCNiAlCo powder was used for the upper heat-resistant layer. The chemical composition of powders is given in Table 1.

Table 1. Chemical analysis of applied materials, wt. %.

Material	Al	Mo	Zr	Nb	Co	Ti	cBN	Ni3Al	SiC	Ta
AlMoNbTaTiZr	28	15	12	15	-	20	-	-	-	10
cBNSiCNiAlCo	-	-	-	-	5	-	40	35	20	-

To improve the functional and mechanical properties of the hybrid composite during HVOF in a protective atmosphere, the AlMoNbTaTiZr and cBNSiCNiAlCo powders were pre-treated by high-energy mechanical processing in the GEFEST-2 (AGO-2U) high-speed planetary ball mill.

HVOF in a protective atmosphere (argon) was chosen as the formation method for surface layers of the composites. This method has several advantages: increased adhesion compared to other methods of gas-thermal spraying, nanoscale structure, and a high speed and productivity of the process. The formation of the composite material was carried out using a multifunctional technological complex for obtaining nanostructured composite surface materials and was processed by means of a single algorithm that combines the following processing cycle (patent number 2718785): high-energy mechanical processing of powders; formation of the functional layer AlMoNbTaTiZr on the surface of the Hastelloy X(NiCrFeMo); formation of the strengthening layer cBNSiCNiAlCo on the surface of the functional layer; and thermal and complex high-temperature thermomechanical processing of the multilayer material. High-temperature thermomechanical processing of the composite AlMoNbTaTiZr-cBNSiCNiAlCo was carried out to increase the strength properties (i.e., to increase the adhesion and cohesion of the composite layers). High-temperature thermomechanical processing included the following: surface plastic deformation of the composite material at 1173–1273 K in a protective atmosphere (argon), which was followed by annealing of the composite material at 1073 K (annealing time 30 min). The surface plastic deformation was carried out by rolling cylindrical samples of the composite materials by rollers.

The formed surface layers of the composition were investigated using metallographic, durometric, X-ray structural and spectral analyses. X-ray phase analysis was carried out on a "Dron-7M" diffractometer in Cu-Kα radiation. The hardness of the composition layers was measured using a Falcon 503 device. The microstructures of the layers were examined on scanning and transmission electron microscopes, JSM-7500F and JEM-2100, respectively.

To assess the quality of the composite layers, we performed mechanical adhesion tests on an Instron 8801 testing machine. Multi-cycle fatigue tests of cylindrical specimens under bending with rotation were performed on MUI-6000 equipment.

To determine the porosity of the composites, we used a hydrostatic method (hydrostatic weighing) [28]; this method is based on the determination of the weight loss of the test composite experienced by the composite when immersed in a liquid. According to the law of Archimedes, this weight loss is equal to the weight of the liquid in the volume of the body. In the measurements, we used pure distilled water, the temperature dependence of which is well known. We used an electronic scale to measure the weight.

We used the pin method to determine the adhesion of surface composites. In the pin method, the basis is a washer, and a pin is installed in the hole in such a way that its end surface is flush with the outer plane of the washer. After preparation, a surface composite is applied to the common surface of the end face of the pin and washer. To prevent it falling out during spraying, the pin is fixed with a screw. The test consists of pulling the pin by applying force P (tensile test, Instron 8801 machine).

3. Results

In the process of high-energy machining (HEM), the powder particles undergo crushing and intense plastic deformation. This leads to a temperature increase and the formation of numerous defects, which are the centers of nanograin formation. Statistical estimation of duration influence of HEM process on size of powder particles allowed for the optimization of the following machining parameters: drum rotation frequency 1800–2000 min^{-1}, driver rotation frequency 800–100 min^{-1}, ball diameter 6 mm, and operating time 15–30 min. The particle size of the AlMoNbTaTiZr powder before HEM ranged from 5 to 20 μm (Figure 2a); after HEM, the size of the AlMoNbTaTiZr powder particles was 1 to 10 μm (Figure 2b). The particle size of the cBNSiCNiAlCo powder before HEM was 8 to 50 μm (Figure 2c); after HEM, the particles of the cBNSiCNiAlCo powder have the size of 1 to 15 μm (Figure 2d).

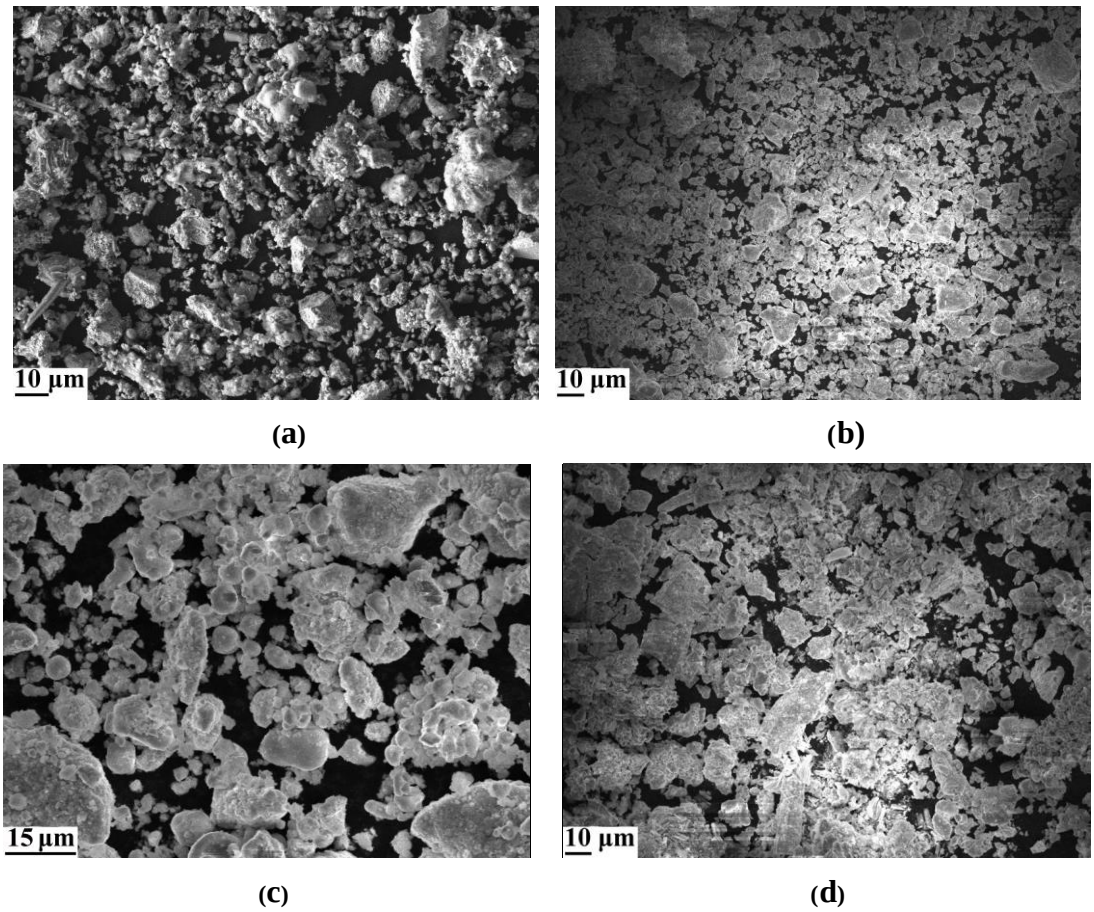

Figure 2. SEM image of the AlMoNbTaTiZr powder before HEM: ×500 (a); after HEM: ×500 (b). The cBNSiCNiAlCo before HEM: ×2500 (c); after HEM: ×600 (d).

Optimal processing modes have been defined by the following criteria: layer thickness and defects (propane consumption 60–85 L/min, oxygen consumption 120–160 L/min; carrier gas consumption (argon) 40–50 L/min; spraying distance 200–300 mm; spraying angle 70–90°; burner speed 1–1.5 m/min; rotation speed of coated part 800–1000 rpm; and residual argon pressure in the chamber 0.8 Pa). After sputtering and machining to size, the samples were annealed in vacuum at T = 1073 K for 2 h.

3.1. Structural and mechanical features of composite materials Hastelloy X (NiCrFeMo)-AlMoNbTaTiZr-cBNSiCNiAlCo

After HVOF in a protective atmosphere and subsequent high-temperature thermomechanical treatment of the Hastelloy X(NiCrFeMo)-AlMoNbTaTiZr-cBNSiCNiAlCo composite, its total thickness was 1.5 mm (the thickness of the AlMoNbTaTiZr layer was 1 mm and the cBNSiCNiAlCo layer was 0.5 mm).

The layers' structure has an extremely weak etchability with conventional reagents. This is largely due to a strong grain refinement as a result of high-speed heating, rapid cooling, and significant deformation (Figure 3). These factors provide special structural effects. Due to HVOF characteristic features and subsequent high-temperature thermomechanical treatment on proprietary equipment (high cooling rate and rapid hardening of the composite), the AlMoNbTaTiZr layer lacks clearly defined columnar dendrites. Thus, the structure can be characterized as nanocrystalline. The complex treatment of the composite (including HEM + HVOF + HTTP) leads to a significant improvement of the layer structure (Figure 3a,b), reduction of porosity (from 2 to 0.1%) and an increase of adhesion and cohesion by 200–230%. The microhardness of the composite was as follows: the Hastelloy X (NiCrFeMo)—3.1 GPa, the AlMoNbTaTiZr—8.7–9.3 GPa, and the cBNSiCNiAlCo—19.2–19.4 GPa. The grain size in the layers of the composite material was as follows: the AlMoNbTaTiZr—53–97 nm (Figure 3c) and the cBNSiCNiAlCo—83–315 nm (Figure 3d).

The results of the X-ray phase analysis showed that the initial phase state of the AlMoNbTaTiZr layer at room temperature is the austenitic B2 and BCC phases (Figure 4a). The main structural components of the hardening layer cBNSiCNiAlCo are BN with a cubic lattice, SiC with a hexagonal lattice, Ni3Al with a cubic lattice, and Co with a cubic lattice (Figure 4b). The diffractogram of the cBNSiCNiAlCo layer corresponds to the diffractogram of a polycrystalline sample, representing a series of peaks on a smooth background line.

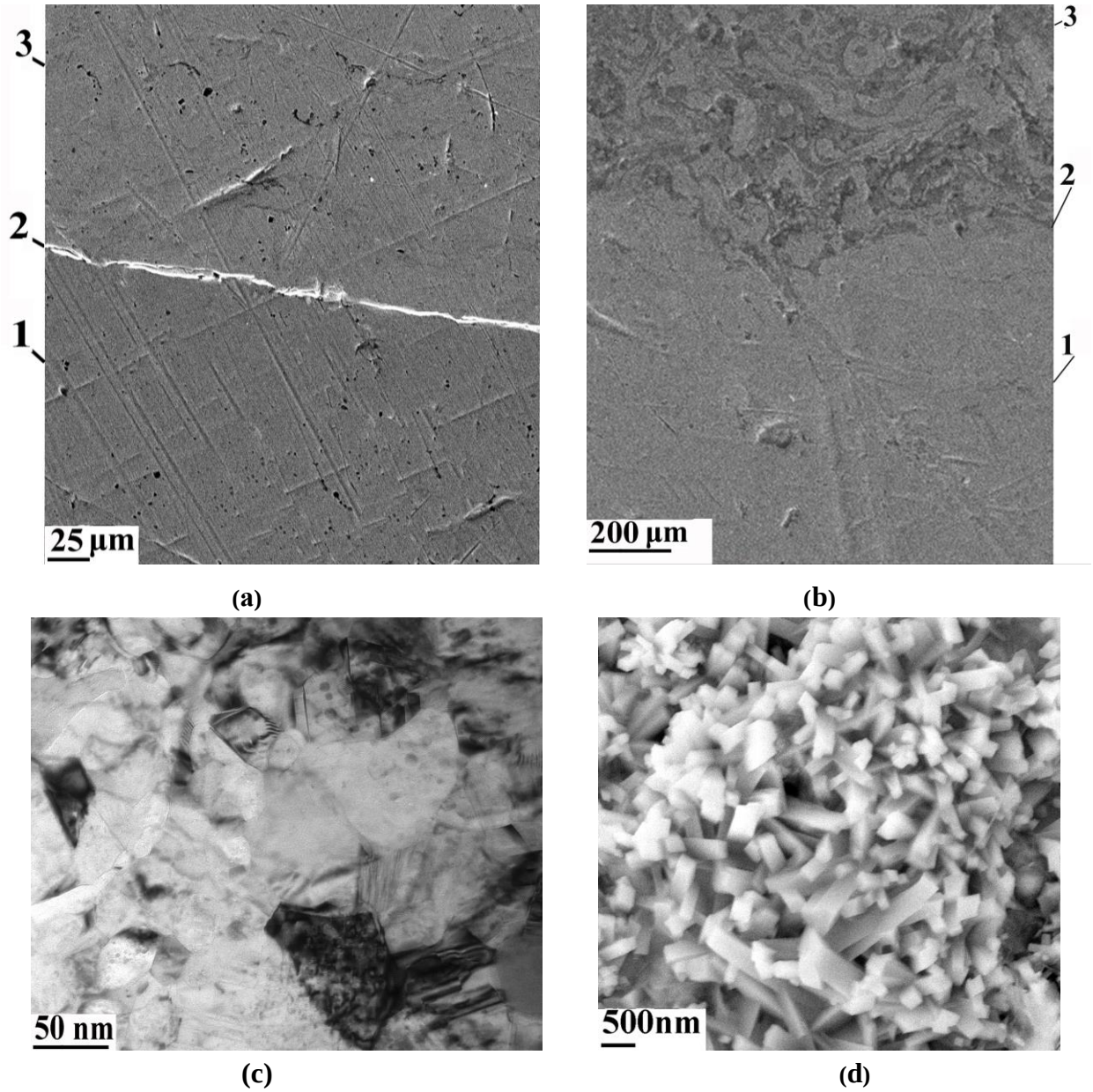

Figure 3. Structure of composite materials Hastelloy X (NiCrFeMo)-AlMoNbTaTiZr-cBNSiCNiAlCo: (a)—the alloy Hastelloy X (NiCrFeMo) (1); the interface between the alloy Hastelloy X (NiCrFeMo) and the layer AlMoNbTaTiZr (2); the layer AlMoNbTaTiZr (3), ×1000. (b)—the AlMoNbTaTiZr layer (1); interface between the AlMoNbTaTiZr and the cBNSiCNiAlCo layers (2); the cBNSiCNiAlCo alloy layer (3), ×1000. (c)—structure of the AlMoNbTaTiZr layer ×100000. (d)—structure of the cBNSiCNiAlCo layer ×10000.

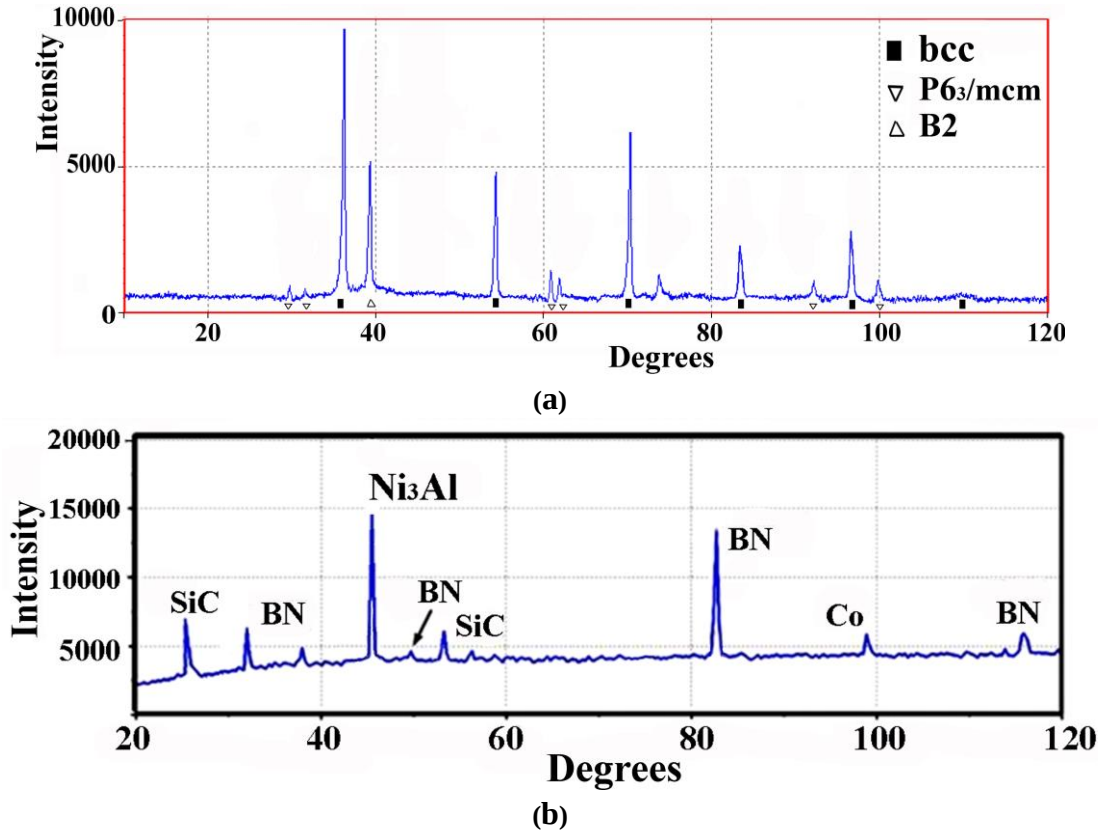

Figure 4. Diffractograms of the composite material AlMoNbTaTiZr-cBNSiCNiAlCo: (a) the layer AlMoNbTaTiZr, (b) the layer cBNSiCNiAlCo.

The parameters of the crystal lattices of the phases included in the composite material AlMoNbTaTiZr-cBNSiCNiAlCo are presented in Table 2.

Table 2. Parameters of crystal lattices of phases included into the composite material.

Phase, lattice type	a, nm	$V_{at} \cdot 10^{-3}$	b, nm	c, nm	β, deg.
AlMoNbTaTiZr					
B2 (face-centered cubic lattice)	0.3032	27.87	-	-	90.00
BCC (volumetric centered cubic lattice)	0.3178	32.1	-	-	90.00
cBNSiCNiAlCo					
BN (cubic)	0.3613	47.16	0.3613	0.3613	90.00
SiC (hexagonal)	0.3096	86.87	0.3096	1.0083	-
Ni3Al (cubic)	0.3574	45.65	0.3574	0.3574	90.00
Co (cubic)	0.3546	44.59	0.3546	0.3546	90.00

4. Discussion

The choice of the composite architecture "Hastelloy X (NiCrFeMo)-AlMoNbTaTiZr-cBNSiCNiAlCo" depends on its functional purpose and practical application. In any case, the surface layers of products are exposed to external forces, temperature, corrosion effects, and must provide durability and survivability in operating conditions. The main factors, which determine the reliability and survivability of the composite, are high adhesion on both the "coating-base" interface and between the layers and the composite material architecture, which prevents the cracks and puts barriers for their propagation.

All technologies of composite layers form the nanostructure under high energy influences. In order to ensure the multifunctionality of the composite layers, it is very important to design its outer layer, which perceives the external impact. To increase wear resistance, the outer layer of the composite should have a high wear resistance. Meanwhile, the underlying layers should provide a high load-bearing capacity, thereby damping characteristics under mechanical or thermal impact. To increase durability and survivability of the product in conditions of either corrosion-fatigue or friction-fatigue cyclic loading, it is necessary to create a surface layer of composite using ceramic the material cBNSiCNiAlCo. This material has a stable high corrosion-fatigue strength, heat resistance and wear resistance in operating conditions. The underlying layer of the composite should have an increased relaxation and damping ability to provide inhibition of developing cracks. As the underlying composite layer, we selected a layer made of the high-entropic material AlMoNbTaTiZr. It has increased strength properties [29,30], reliable adhesion, and cohesion under operating conditions.

In the process of high-temperature thermomechanical processing of the Hastelloy X (NiCrFeMo)-AlMoNbTaTiZr-cBNSiCNiAlCo composite material, its surface layers undergo intense plastic deformation and high heating temperature. Temperature exposure forms numerous defects, amorphous and nanograin structure. Furthermore, in the process of high-temperature thermomechanical processing, the surface layers of the composite experience large contact influences during roller loading. This leads to micro-welding of the boundary layers of the Hastelloy X (NiCrFeMo)-AlMoNbTaTiZr and the AlMoNbTaTiZr-cBNSiCNiAlCo composite. In turn, this causes an increase of adhesion and cohesion of composite layers.

Severe plastic deformation of composite layers takes place in the process of high-temperature thermomechanical processing, which includes the stages of intense deformation, polygonization and recrystallization. The formed nanostructured particles of the composite layers in the process of deformation experience high contact pressures, first leading to the deformation of the particles of the composite layers, and then to the diffusion of the particles into the base material (Hastelloy X alloy) and their subsequent splicing. In the same way, there is an increase in cohesion between the AlMoNbTaTiZr and the cBNSiCNiAlCo layers. Crystallization during high-temperature thermomechanical treatment is accompanied by the formation of nuclei on long-range order fluctuations, the number and size of which is determined by the degree of cooling. When the composite layers are cooled, crystallization proceeds under conditions of heat deficiency and the temperature at the front of the growing crystal drops sharply. This leads to a suspension of crystal growth at a certain stage, and to the melt, which remains untransformed, solidifies with the formation of an amorphous state. The amorphous component undergoing hot plastic deformation subsequently undergoes dynamic recrystallization with the formation of a nanostructure.

4.1. Performance properties of composites

Composites are generally known for their unique strength properties, their wear and corrosion resistance [31,32]. These alloys can be presented in various forms. They demonstrate high resistance under conditions of cyclic loading, whether in the form of wires, strips or bands. Stress values of composite amplitude have worked out 10^7 cycles at an amplitude of alternating stresses close to endurance limit (σ_{-1}) for the Hastelloy X (NiCrFeMo) are 340 MPa. This is the value for composite surface layers AlMoNbTaTiZr-cBNSiCNiAlCo—453 MPa, AlCoCrCuFeNi-cBNCoMo—410 MPa, and AlCoCrCuFeNi-B4CCoMo—385 MPa (Figure 5a). As a result of multicyclic fatigue tests at bending with rotation (Figure 4), it has been established that the greatest cyclic durability belongs to the Hastelloy X (NiCrFeMo)-AlMoNbTaTiZr-cBNSiCNiAlCo composite (Figure 5a, curve 4). Its endurance limit at symmetrical cycle σ_{-1} = 453 MPa, and the lowest Hastelloy X (NiCrFeMo) with endurance limit at symmetrical cycle σ_{-1} = 340 MPa (Figure 5a, curve 4).

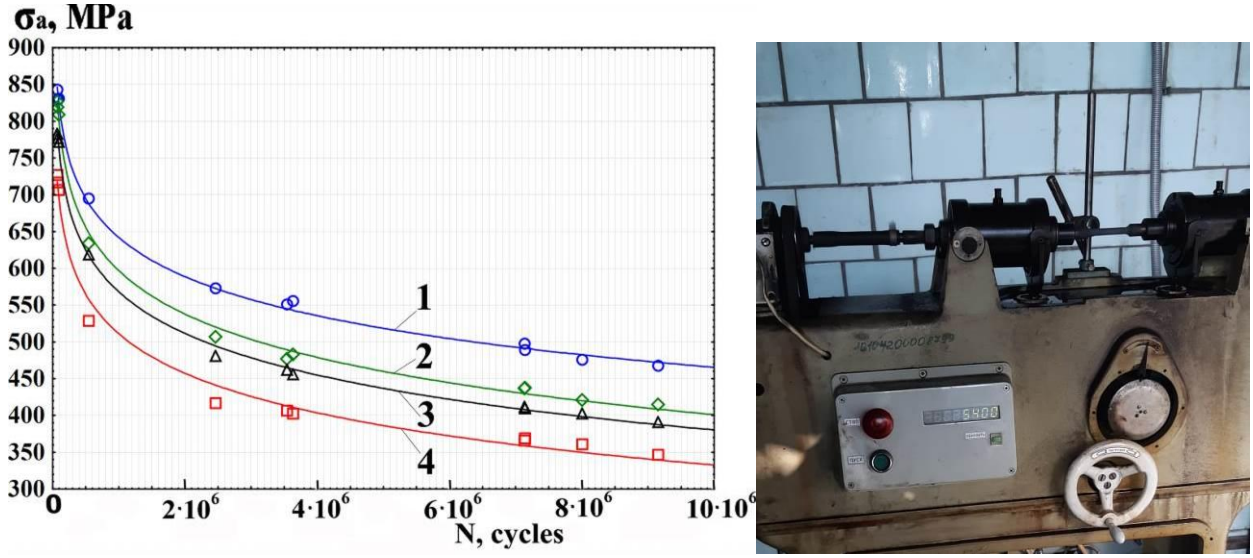

(a) **(b)**

Figure 5. Multi-cycle fatigue curves: the Hastelloy X (NiCrFeMo) (4), the Hastelloy X (NiCrFeMo)-AlMoNbTaTiZr-cBNSiCNiAlCo ($\delta \approx 1.5$ mm) (1); the Hastelloy X (NiCrFeMo)-AlCoCrCuFeNi-cBNCoMo ($\delta \approx 1.5$ mm) (2); the Hastelloy X (NiCrFeMo)-AlCoCrCuFeNi-B4CCoMo ($\delta \approx 1.5$ mm) (3)-(a); Photograph of fatigue tests of composite specimens, on bending with rotation-(b).

The tests results of samples made of the Hastelloy X (NiCrFeMo) alloy (Figure 5a, curve 4) and after surface modification of the Hastelloy X (NiCrFeMo) with composites (Figure 5a, curves 1–3) show that surface modification slows down the damage accumulation process and increases endurance limit of the Hastelloy X (NiCrFeMo).

This explains the mechanism of deformation of the composite material, which occurs during high-temperature thermomechanical processing. An increase in the durability of the Hastelloy X (NiCrFeMo) samples with the AlMoNbTaTiZr and cBNSiCNiAlCo composite layers is explained as the features of the destruction of nanostructured materials (consisting in the inhibition of destruction

at grain boundaries, preventing branching and crack movement due to strengthening of the boundaries). Additionally, due to the following peculiarities of layered composites (different properties of the composite layers: mechanical properties, Young and Shear moduli, greater energy absorption than single-layer materials), and each layer of the surface composite acts as a "barrier" during crack growth (crack growth slows down).

In terms of material structure, fatigue strength is primarily determined by the energy required for crack nucleation and the rate of crack propagation. HVOF and the subsequent combined treatment of the resulting composite, as a means of modifying the surface layers, primarily affects the process of microcrack initiation. The mechanism of this influence is probably related both to the nanostructuring of the surface layers, and to the peculiarities of the chemical and phase composition of the high-entropic layer.

The stressamplitude (σ_a) as a function of cyclic durability (N) changes according to polynomial dependence (Figure 4a) and is described by empirical Eqs 1–4, obtained from the mathematical analysis of experimental data in Statistica v10.0 software:

-Hastelloy X (NiCrFeMo)-AlMoNbTaTiZr-cBNSiCNiAlCo:

$$\sigma_a = 811 - 9.07 \times 10^{-5} \times N + 5.85 \times 10^{-12} \times N^2, \text{(MPa)}, \quad (1)$$

-Hastelloy X (NiCrFeMo):

$$\sigma_a = 682 - 9.94 \times 10^{-5} \times N + 6.96 \times 10^{-12} \times N^2, \text{(MPa)}, \quad (2)$$

-Hastelloy X (NiCrFeMo)-AlCoCrCuFeNi-cBNCoMo:

$$\sigma_a = 785.95 - 10^{-4} \times N + 7.52 \times 10^{-12} \times N^2, \text{(MPa)}, \quad (3)$$

-Hastelloy X (NiCrFeMo)-AlCoCrCuFeNi-B4CCoMo:

$$\sigma_a = 750.31 - 10^{-4} \times N + 7.11 \times 10^{-12} \times N^2, \text{(MPa)}, \quad (4)$$

where σ_a is stress amplitude (MPa);

N-cyclic durability (cycle).

5. Conclusions

The conducted research shows that the task of ensuring the reliability of details, units and assemblies working in the oil and gas industry, can be successfully solved by functionally oriented multi-component surface composites. These composites should include a layer of a high-entropic alloy and a surface layer of a combined ceramic heat-resistant alloy.

We proposed a technology of layer-by-layer composite synthesis, with a subsequent high-temperature thermomechanical treatment in argon medium. We implemented this technology on the patented equipment (patent № 2718785) in a single technological cycle, which determines not only novelty, but also economic feasibility of technical solutions.

The proposed technology allowed to increase the adhesive strength of the surface composite by 200–230%, reduce the composite porosity to 0.1% and improve the functional and operational properties of composites. This technology included high-energy mechanical processing, HVOF in a protective atmosphere, subsequent high-temperature thermomechanical and thermal processing of the composite in a protective atmosphere.

Based on the complex X-ray structural and electron microscopic investigations, we determined the structural parameters of the surface composites. We have shown that the alloy AlMoNbTaTiZr, has a nanocrystalline structure with a grain size of 53–97 nm, and the alloy cBNSiCNiAlCo consists of many intermetallic phases and inclusions, and has a structure with a grain size of 83–315 nm.

We studied the microhardness of the composite Hastelloy X (NiCrFeMo)-AlMoNbTaTiZr-cBNSiCNiAlCo. The results demonstrated that the application of high-temperature thermomechanical processing increases microhardness of the composite.

As a result of experimental data processing, we compiled the empirical mathematical dependences of the stress amplitude on the cyclic durability. We performed mechanical tests of the composites Hastelloy X (NiCrFeMo)-AlMoNbTaTiZr-cBNSiCNiAlCo, the Hastelloy X (NiCrFeMo)-AlCoCrCuFeNi-cBNCoMo, the Hastelloy X (NiCrFeMo)-AlCoCrCuFeNi-B4CCoMo for multicycle fatigue under bending with rotation. The tests have shown that the Hastelloy X (NiCrFeMo)-AlMoNbTaTiZr-cBNSiCNiAlCo composite with a stress amplitude σ_a = 453 MPa at cyclic durability $N = 1.15 \times 10^7$ cycles has the greatest cyclic durability.

Use of AI tools declaration

The authors declare they have not used Artificial Intelligence (AI) tools in the creation of this article.

Author Contributions

Conceptualization, P. Rusinov and Z. Blednova; methodology, P. Rusinov, Z. Blednova, A. Rusinova, G. Kurapov; software, P. Rusinov, A. Rusinova, G. Kurapov, M. Semadeni; validation, P. Rusinov, Z. Blednova, A. Rusinova, G. Kurapov, M. Semadeni; formal analysis, P. Rusinov, A. Rusinova, G. Kurapov; investigation, P. Rusinov, Z. Blednova; resources, P. Rusinov, A. Rusinova, G, Kurapov, M. Semadeni; data curation, P. Rusinov, A. Rusinova, G. Kurapov; writing original draft preparation, P. Rusinov; writing review and editing, P. Rusinov and Z. Blednova; visualization, G, Kurapov, M. Semadeni; supervision, P. Rusinov, A. Rusinova, G. Kurapov; project administration, P. Rusinov; funding acquisition, P. Rusinov. All authors have read and agreed to the published version of the manuscript.

Funding

This research was funded by Russian Science Foundation, grant number 23-23-00074.

Conflicts of interest

The authors declare no conflict of interest.

References

1. Shen JJ, Gonçalves R, Choi YT, et al. (2023) Microstructure and mechanical properties of gas metal arc welded CoCrFeMnNi joints using a 308 stainless steel filler metal. *Scripta Mater* 222: 115053. https://doi.org/10.1016/j.scriptamat.2022.115053
2. Shen JJ, Agrawal P, Rodrigues TA, et al. (2022) Gas tungsten arc welding of as-cast $AlCoCrFeNi_{2.1}$ eutectic high entropy alloy. *Mater Design* 223: 111176. https://doi.org/10.1016/j.matdes.2022.111176
3. Li BQ, Wang L, Wang BB, et al. (2022) Electron beam freeform fabrication of NiTi shape memory alloys: Crystallography, martensitic transformation, and functional response. *Mater Sci Eng A* 2022: 143135. https://doi.org/10.1016/j.msea.2022.143135
4. Felice IO, Shen JJ, Barragan A, et al. (2023) Wire and arc additive manufacturing of Fe-based shape memory alloys: Microstructure, mechanical and functional behavior. *Mater Design* 231: 112004. https://doi.org/10.1016/j.matdes.2023.112004
5. Yusuf SM, Cutler S, Gao N (2019) Review: The impact of metal additive manufacturing on the aerospace industry. *Metal* 9: 1286. https://doi.org/10.3390/met9121286
6. Makhutov NA, Matvienko YG, Blednova ZM, et al. (2022) The effect of surface coating by shape memory alloys on mechanical properties of steel. *Fatigue Fract Eng M* 45: 1550–1553. https://doi.org/10.1111/ffe.13672
7. Tang H, Tao W, Wang H, et al. (2018) High-performance infrared emissivity of micro-arc oxidation coatings formed on titanium alloy for aerospace applications. *Int J Appl Ceram Tec* 15: 579–591. https://doi.org/10.1111/ijac.12861
8. Bhutta MU, Khan ZA (2020) Wear and friction performance evaluation of nickel based nanocomposite coatings under refrigerant lubrication. *Tribol Int* 148: 106312. https://doi.org/10.1016/j.triboint.2020.106312
9. Segura-Cardenas E, Ramirez-Cedillo EG, Sandoval-Robles JA, et al. (2017) Permeability study of austenitic stainless steel surfaces produced by selective laser melting. *Metals* 7: 521. https://doi.org/10.3390/met7120521
10. Haro EE, Odeshi AG, Szpunar JA (2016) The energy absorption behavior of hybrid composite laminates containing nano-fillers under ballistic impact. *Int J Impact Eng* 96: 11–22. https://doi.org/10.1016/j.ijimpeng.2016.05.012
11. Mishnaevsky LJR (2019) Toolbox for optimizing anti-erosion protective coatings of wind turbine blades: Overview of mechanisms and technical solutions. *Wind Energy* 22: 1636–1653. https://doi.org/10.1002/we.2378
12. Ahmadnia A (2000) *Energy Absorption of Macrocomposite Laminates*, London: Queen Mary University of London. http://qmro.qmul.ac.uk/xmlui/handle/123456789/1342
13. Wadsworth J, Lesuer DR (2000) Ancient and modern laminated composites—from the great pyramid of gizeh to Y2K. *Mater Charact* 45: 289–313. https://doi.org/10.1016/S1044-5803(00)00077-2
14. Sun MY, Bai YH, Li MX, et al. (2018) Structural design and energy absorption mechanism of laminated SiC/BN ceramics. *J Eur Ceram Soc* 38: 3742–3751. https://doi.org/10.1016/j.jeurceramsoc.2018.04.052

15. Naidoo LC, Fatoba O, Akinlabi S, et al. (2020) Material characterization and corrosion behavior of hybrid coating Ti-Al-Si-Cu/Ti-6Al-4V composite. *Materialwiss Werkstofftech* 51: 766–773. https://doi.org/10.1002/mawe.202000019
16. Rusinov PO, Blednova ZM, Kurapov GV (2023) Functionally oriented composite layered materials with martensitic transformations. *Surf Innov* 11: 26–37. https://doi.org/10.1680/jsuin.21.00077
17. Anand EE, Natarajan S (2015) Effect of carbon nanotubes on corrosion and tribological properties of pulse-electrodeposited Co-W composite coatings. *J Mater Eng Perform* 24: 128–135. https://doi.org/10.1007/s11665-014-1306-z
18. Rusinov PO, Blednova ZM, Rusinova AA, et al. (2023) Development and Research of New Hybrid Composites in Order to Increase Reliability and Durability of Structural Elements. *Metals* 13: 1177. https://doi.org/10.3390/met13071177
19. Xiong JJ, Zhu YT, Luo CY, et al. (2021) Fatigue-driven failure criterion for progressive damage modelling and fatigue life prediction of composite structures. *Int J Fatigue* 145: 106110. https://doi.org/10.1016/j.ijfatigue.2020.106110
20. Kong WW, Yuan C, Zhang BN (2020) Investigations on cyclic deformation behaviors and corresponding failure modes of a Ni-Based superalloy. *Mater Sci Eng A* 791: 139775. https://doi.org/10.1016/j.msea.2020.139775
21. Cho H, Nam S, Hwang I, et al. (2019) Fatigue behaviors of resistance spot welds for 980 MPa grade TRIP steel. *Metals* 9: 1086. https://doi.org/10.3390/met9101086
22. Su ZM, Lin PC, Lai WJ, et al. (2020) Fatigue analyses and life predictions of laser-welded lap-shear specimens made of low carbon and high strength low alloy steels. *Int J Fatigue* 140: 105849. https://doi.org/10.1016/j.ijfatigue.2020.105849
23. Watanabe H, Murata T, Nakamura S, et al. (2021) Effect of cold-working on phase formation during heat treatment in CrMnFeCoNi system high-entropy alloys with Al addition. *J Alloys Compd* 872: 159668. https://doi.org/10.1016/j.jallcom.2021.159668
24. Wang M, Huang MX (2020) Abnormal TRIP effect on the work hardening behavior of a quenching and partitioning steel at high strain rate. *Acta Mater* 188: 551–559. https://doi.org/10.1016/j.actamat.2020.02.035
25. Behravan A, Zarei-Hanzaki A, Fatemi SM, et al. (2019) The effect of aging temperature on microstructure and tensile properties of a novel designed Fe-12Mn-3Ni Maraging-TRIP steel. *Steel Research Int* 90: 1800282. https://doi.org/10.1002/srin.201800282
26. Tan XD, He HS, Lu WJ, et al. (2020) Effect of matrix structures on TRIP effect and mechanical properties of low-C low-Si Al-added hot-rolled TRIP steels. *Mater Sci Eng A* 771: 138629. https://doi.org/10.1016/j.msea.2019.138629
27. Yang J, Jo YH, Kim DW, et al. (2020) Effects of transformation-induced plasticity (TRIP) on tensile property improvement of $Fe_{45}Co_{30}Cr_{10}V_{10}Ni_{5-x}Mn_x$ high-entropy alloys. *Mater Sci Eng A* 772: 138809. https://doi.org/10.1016/j.msea.2019.138809
28. Isakaev EK, Mordynsky VB, Sidorova EV, et al. (2011) Comparative analysis of methods for measuring the porosity of gas-thermal coatings. *Eng technol* 3: 25–30. http://www.ltc.ru/newsltc/2/1009_1.shtml
29. Kustas AB, Jones MR, DelRio FW, et al. (2022) Extreme hardness at high temperature with a lightweight additively manufactured multi-principal element superalloy. *Appl Mater Today* 29: 101669. https://doi.org/10.1016/j.apmt.2022.101669

30. Whitfield TE, Stone HJ, Jones CN, et al. (2021) Microstructural degradation of the $AlMo_{0.5}NbTa_{0.5}TiZr$ refractory metal high-entropy superalloy at elevated temperatures. *Entropy* 23: 80. https://doi.org/10.3390/e23010080
31. Rusinov PO, Blednova, ZM (2022) Study of the structure and properties of a high-entropy ceramic composite material. *Surf Innov* 10: 217–226. https://doi.org/10.1680/jsuin.21.00047
32. Zhao YC, Zhao PB, Li WS, et al. (2019) The microalloying effect of Ce on the mechanical properties of medium entropy bulk metallic glass composites. *Crystals* 9: 483. https://doi.org/10.3390/cryst9090483